Influence of Nonuniform Particle Temperature on the Radiatively Active Particle Ignition

Seung Wook Baek*
Korea Advanced Institute of Science and Technology, Seoul, Korea

Introduction

IN the area of fire safety there has been a growing interest in the conditions under which a reactive two-phase mixture can thermally ignite. They are usually governed by the conductive and convective heat transfer mechanisms from a thermal source toward two-phase mixture. But radiation sometimes plays a significant role in particle ignition.[1] In a previous paper,[1] the thermal ignition of a two-phase mixture comprised of carbon particles and air in a slab geometry has been analyzed to determine the effects of radiation, particle size, equivalence ratio, and wall temperature. Unlike the previous attempts,[2-4] a less constrained model was used for both the solid and the gas phase.[5]

The former study[1] has shown that the carbon particles located far away from the hot wall are heated up faster than the air due to the far-reaching effect of the radiation. Therefore, radiation causes the carbon particle to be ignited earlier than otherwise. The change of particle size at a fixed carbon mass loading exerted a strong influence such that the larger the particle size, the longer is the ignition delay. However, the carbon mass loading was shown to have a negligible effect on the ignition delays. An appreciable change in the lower wall temperature made no noticeable difference in ignition delays.

The objective of the present article is to investigate the effect of the nonuniformity of the interior particle temperature on the particle ignition as an extension of the former study.[1] In addition, the effects of albedo and wall emissivity, which were not discussed before, are also examined here.

Formulation

To study the effect of the nonuniform particle temperature in the system as schematized in Fig. 1, the main assumptions are as follows:

1) The system is one-dimensional.
2) The mixture of air and carbon particles remains quiescent.
3) The shape of carbon particles is assumed to be spherical and these particles are uniformly monodispersed in space.
4) The volume occupied by particles is negligible compared with the gas suspension volume.
5) The carbon particles with constant monochromatic radiative properties are supposed to absorb and emit, as well as isotropically scatter the radiation.
6) Both opaque walls are assumed to be diffuse reflectors and emitters.

The energy equation for the gas phase can be cast in the same form as before

$$\rho_g C_g \frac{\partial T_g}{\partial t} = \lambda_g \frac{\partial^2 T_g}{\partial x^2} - nQ \tag{1}$$

Received Sept. 25, 1990; revision received Jan. 7, 1991; presented as Paper 91-0483 at the AIAA 29th Aerospace Sciences Meeting, Reno, NV, Jan. 7-10, 1991; accepted for publication Feb. 25, 1991.
Copyright © 1991 by the American Institute of Aeronautics and Astronautics, Inc. All rights reserved.
*Associate Professor, Department of Aerospace Engineering. Member AIAA.

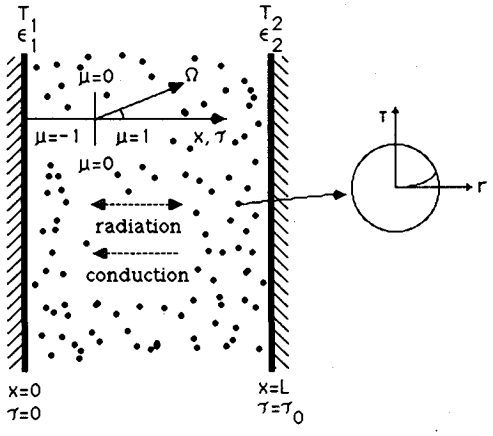

Fig. 1 Schematic diagram of the physical system.

where T_g is the gas phase temperature and λ_g(0.0628 W/mK), ρ_g(0.392 kg/m^3), and C_g(1.122 kJ/kgK) are the thermal conductivity, density, and specific heat of the gas, respectively. The particle number density is denoted by n. The amount of heat transferred between gas and one particle Q is given by

$$Q = \pi D_c^2 h(T_g - T_c|_{r=D_c/2}) \tag{2}$$

where D_c is the particle diameter and r is the radial coordinate inside the particle. $T_c(r=D_c/2)$ is the particle surface temperature, which will hereafter be denoted by T_{cs}. Since the mixture of air and carbon particles is assumed to reside quiescently, the convective heat transfer coefficient h can be estimated using the following equation

$$Nu = \frac{hD_c}{\lambda_g} = 2 \tag{3}$$

To determine the temperature distribution inside the particle, the thermal interactions between air and particles need to be taken into account. Here the interior particle temperature distribution is assumed to be spherically symmetric so that the thermal equation inside a carbon particle is given by

$$\rho_c C_c \frac{\partial T_c}{\partial t} = \frac{\lambda_c}{r^2} \frac{\partial}{\partial r}\left(r^2 \frac{\partial T_c}{\partial r}\right) \tag{4}$$

where λ_c(0.886 W/mK), ρ_c(1200 kg/m^3), and C_c(1.794 kJ/kgK) are the thermal conductivity, density, and specific heat of the carbon particle. The corresponding boundary conditions are

$$\text{at } r = \frac{D_c}{2}: \quad \lambda_c \frac{\partial T_c}{\partial r}\Big|_{r=D_c/2} = h(T_g - T_{cs}) + q_r + qH$$
$$\text{at } r = 0: \quad \frac{\partial T_c}{\partial r} = 0 \tag{5}$$

where H is the heat of combustion per unit mass of carbon. The local radiative heat flux toward the particle surface is denoted by q_r. The rate of consumption of carbon per unit external geometric surface q can be expressed as follows[6]:

$$q = \frac{P_{O_2}}{1/k_s + 1/k_d} \tag{6}$$

in terms of the oxygen pressure P_{O_2}, the surface reaction rate coefficient k_s, and the corrected form of the diffusional reaction rate coefficient k_d as proposed in Baek and Seung.[7] By introducing the following dimensionless variables

$$\theta_g = T_g/T_2, \quad \alpha_g = \lambda_g/(\rho_g C_g), \quad \tau = \beta x, \quad t^* = \alpha_g \beta^2 t,$$
$$\theta_c = T_c(r)/T_2, \quad \theta_{cs} = T_{cs}/T_2, \quad N_1 = n\pi D_c^2 h/(\beta^2 \lambda_g) \tag{7}$$

Equation (1) can be transformed to

$$\frac{\partial \theta_g}{\partial t^*} = \frac{\partial^2 \theta_g}{\partial \tau^2} - N_1(\theta_g - \theta_{cs}) \tag{8}$$

In Eq. (7) τ is the optical thickness by definition and the extinction coefficient is denoted by $\beta = \alpha_a + \sigma_s$ where α_a and σ_s are the absorption coefficient and scattering coefficient, respectively. A radiation model for the radiative heat flux q_r is required in order to make Eq. (5) tractable.

With dimensionless variables

$$\psi(\tau) = \frac{G(\tau)}{\sigma T_2^4}, \quad X = \frac{B}{\sigma T_2^4} \tag{9}$$

the following equations are obtained:

$$q_r(\tau) = 2\sigma T_2^4 \left[X_1 E_3(\tau) - X_2 E_3(\tau_0 - \tau) + \int_0^\tau \cdot \left\{ (1 - \omega_a)\theta_{cs}^4(\eta) + \frac{\omega_a}{4}\psi(\eta) \right\} E_2(\tau - \eta)\mathrm{d}\eta - \int_\tau^{\tau_0} \cdot \left\{ (1 - \omega_a)\theta_{cs}^4(\eta) + \frac{\omega_a}{4}\psi(\eta) \right\} E_2(\eta - \tau)\mathrm{d}\eta \right] \tag{10}$$

$$\psi(\tau) = 2X_1 E_2(\tau) + 2X_2 E_2(\tau_0 - \tau) + 2\int_0^{\tau_0} \cdot \left[(1 - \omega_a)\theta_{cs}^4(\eta) + \frac{\omega_a}{4}\psi(\eta) \right] E_1(|\tau - \eta|)\mathrm{d}\eta \tag{11}$$

$$X_1 = \varepsilon_1 \theta_1^4 + 2(1 - \varepsilon_1)\left\{ X_2 E_3(\tau_0) + \int_0^{\tau_0} \cdot \left[(1 - \omega_a)\theta_{cs}^4(\eta) + \frac{\omega_a}{4}\psi(\eta) \right] E_2(\eta)\mathrm{d}\eta \right\} \tag{12}$$

and

$$X_2 = \varepsilon_2 + 2(1 - \varepsilon_2)\left\{ X_1 E_3(\tau_0) + \int_0^{\tau_0} \cdot \left[(1 - \omega_a)\theta_{cs}^4(\eta) + \frac{\omega_a}{4}\psi(\eta) \right] E_2(\tau_0 - \eta)\mathrm{d}\eta \right\} \tag{13}$$

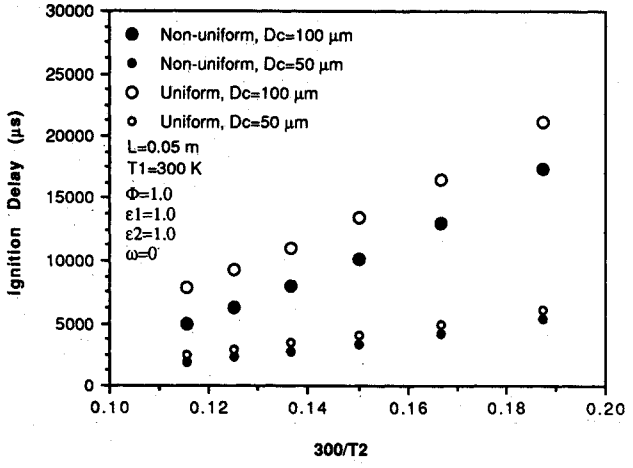

Fig. 2 Effect of nonuniform particle temperature on ignition delays for two particle sizes, D_c = 50 and 100 μm, with Φ = 1.0, L = 0.05 m, T_1 = 300 K, T_2 = 2000 K, $\varepsilon_1 = \varepsilon_2$ = 1.0, and nonscattering case (ω_a = 0).

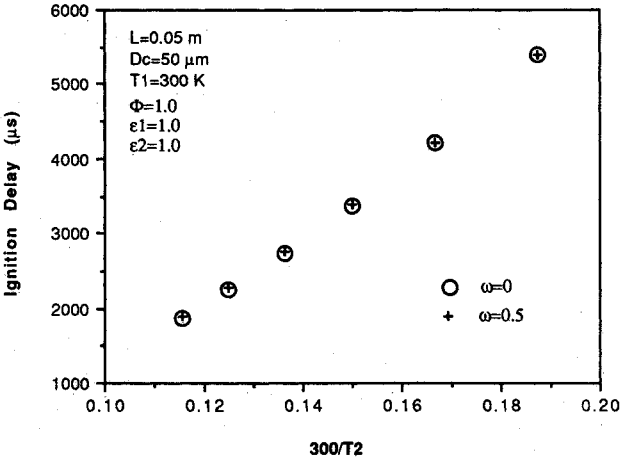

Fig. 3 Effect of albedo ω_a on ignition delays for Φ = 1.0, L = 0.05 m, D_c = 50 μm, T_1 = 300 K, and $\varepsilon_1 = \varepsilon_2$ = 1.0.

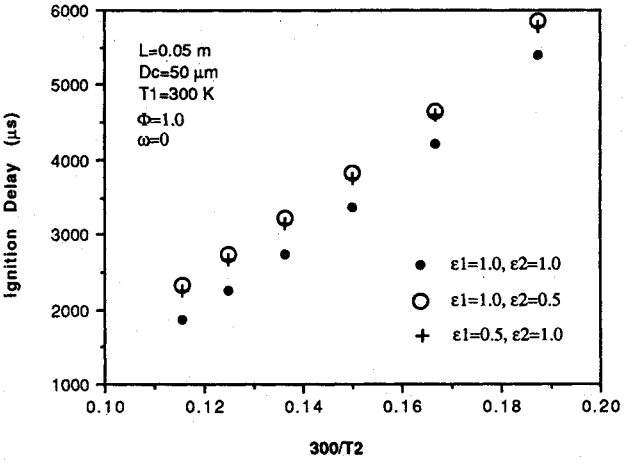

Fig. 4 Effect of cold and hot wall emissivities ε_1 and ε_2 on ignition delays for Φ = 1.0, L = 0.05 m, D_c = 50 μm, T_1 = 300 K, and ω_a = 0.

where $\theta_1 = T_1/T_2$, $\tau_0 = \beta L$ and σ is the Stefan-Boltzmann constant. B_1 and B_2 are the surface radiosities at the left wall ($x = 0, \tau = 0$) and the right wall ($x = L, \tau = \tau_0$), respectively. $E_n(x)$ and $G(\tau)$ are the exponential integral function and the incident radiation, respectively. ε is the surface emissivity and the albedo ω_a is given by $\omega_a = 1 - \alpha_a/\beta$.

The extinction coefficient β is set to be $\beta = 0.21\, n\pi D_c^2$ following Krazinski et al.,[8] since it would be proportional to the local total particle surface area. The boundary conditions are $\theta_g(0,t^*) = \theta_1$ and $\theta_g(\tau_0, t^*) = 1$ and the initial conditions are $\theta_g(\tau, t^* = 0) = \theta_c(r, t^* = 0) = 300/T_2$.

Since the energy equation [Eq. (8)] for the gas phase and the thermal equation [Eq. (4)] for the interior particle temperature with supplementary equations [Eqs. (2),(3),(6),(10–13)] are nonlinearly coupled to one another, a numerical method is chosen to unravel them simultaneously. The grid size and time step were varied until the accuracy of ignition time was within 0.5% of the final value.

Results and Discussion

Unless otherwise specified, the entire calculation presented below was carried out for the following conditions: the left wall temperature T_1 = 300 K, the distance between two walls L = 0.05 m, the emissivities of both walls $\varepsilon_1 = \varepsilon_2 = 1$, the scattering coefficient of radiating medium $\sigma_s = 0$ ($\omega_a = 0$) and the equivalence ratio $\Phi = 1$.

The unsteady solution of the air and carbon particle temperatures was continued until the ignition was detected. Fol-

lowing the reasoning cited in Ref. 1, the ignition is considered to occur when the carbon particle surface at the first grid point from the hot wall reaches the temperature of 1000 K.

For the physical conditions of $\Phi = 1.0$ and two particle sizes, $D_c = 50$ and 100 μm, the effect of nonuniform interior particle temperature on the ignition delays is plotted in Fig. 2 versus the inverse of six hot wall temperatures T_2 nondimensionalized by the initial temperature 300 K. As was expected generally, the ignition delay time decreases with increasing hot wall temperature T_2 and decreasing the particle size D_c. Furthermore, the ignition delays for the case of nonuniform interior particle temperature are shorter than those for the case of uniform particle temperature. This reduction in ignition delays for the case of nonuniform particle temperature is more obvious for the larger particles. For the particle size of $D_c = 50$ μm the decrease in ignition delays is 657 μs at $T_2 = 2600$ K and 688 μs at $T_2 = 1600$ K. Eventually the assumption of uniform particle temperature would result in 35% error at 2600 K and 12.8% error at 1600 K in predicting ignition delays. For the larger particle size of $D_c = 100$ μm the situation turns out to be even worse. The reduction in ignition delays is 2830 μs at $T_2 = 2600$ K and 3835 μs at $T_2 = 1600$ K. This amounts to 56.9% error at $T_2 = 2600$ K and 22.1% error at $T_2 = 1600$ K. Therefore, the larger the particle size, the more error in estimating the ignition delays the assumption of uniformity of the particle temperature would invoke. It results from the fact that the ratio of volume of a spherical particle to surface area is proportional to the particle radius. It means that as the particle size increases, so does the volume-to-surface-area ratio. Since under the assumption of uniformity of the particle temperature the heat transferred from the air to the carbon particle surface is equally distributed throughout the entire particle volume, the whole temperature for the larger particle size would be lowered as much compared with the surface temperature for the condition of nonuniformity of the particle temperature.

Figure 3 shows a negligible effect of the albedo ω_a on the ignition delays with no change in the other given parameters. The ignition delay is seen to increase only 15 μs at $T_2 = 2600$ K and 17 μs at $T_2 = 1600$ K as the albedo increases from $\omega_a = 0$ to 0.5. It results from the fact that the influence of the albedo on the temporal change in the particle surface temperature is almost unnoticeable such that a maximal temperature difference at a given time is just 6 K between two cases $\omega_a = 0$ and 0.5. Physically the albedo represents the fraction of the incident radiation that has not been transformed into thermal energy, i.e., scattered into all directions. In the vicinity of the hot wall, the particle surface temperature for $\omega_a = 0.5$ becomes a little lower than that for $\omega_a = 0$, since the locally incident radiation would be less converted to the thermal energy. But in the region near the cold wall the particle surface temperature for $\omega_a = 0.5$ becomes a little higher than that for $\omega_a = 0$, since the radiation scattered near the hot wall would be transformed to the thermal energy herein. As was noted in Baek and Lee,[9] the influence of the albedo would increase as the optical thickness increases.

The effect of the cold and hot wall emissivities ε_1 and ε_2 on the ignition delays is represented in Fig. 4 for $\Phi = 1.0$, $L = 0.05$ m, $D_c = 50$ μm, $T_1 = 300$ K, and $\omega_a = 0$. The ignition delays corresponding to the black wall emissivities $\varepsilon_1 = \varepsilon_2 = 1.0$ are denoted by the solid circles. When only the hot wall emissivity ε_2 is reduced to 0.5 from 1.0 (denoted by open circles), the ignition delay increases 464 μs at $T_2 = 1600$ K and 460 μs at $T_2 = 2600$ K. The decrease in the hot wall emissivity ε_2 accompanies two counterbalancing effects in the normalized radiosity X_2 in Eq. (13), i.e., the decrease in the emission from the hot wall, which is represented by the first term in Eq. (13), and the increase in the reflection of the emission coming from the cold wall, which is represented by the second term in Eq. (13). Because the former is dominant over the latter, the resulting emission from the hot wall is therefore reduced as ε_2 decreases. The third term in Eq. (13) represents the radiative contribution originating from the carbon particles contained between two walls. When only the cold wall emissivity ε_1 is reduced to 0.5 from 1.0 (denoted by +), the ignition delay increases 401 μs at $T_2 = 1600$ K and 390 μs at $T_2 = 2600$ K, which is less than before. The same physical explanation as before still applies for the normalized radiosity X_1 in Eq. (12). But the change in the hot wall emissivity ε_2 is found to be more influential in predicting the ignition delays.

References

[1]Baek, S. W., "Ignition of Particle Suspensions in Slab Geometry," *Combusion and Flame*, Vol. 81, Sept. 1990, pp. 366–377.

[2]Khalil, H., Shultis, J. K., and Lester, T. W., "Stationary Thermal Ignition of Particle Suspensions," *Journal of Heat Transfer*, Vol. 105, May 1983, pp. 288–294.

[3]Khalil, H., Shultis, J. K., and Lester, T. W., "Ignition of Particle Suspensions by Radiant Emission from Bounding Walls," *Combustion and Flame*, Vol. 53, Nov. 1983, pp. 149–152.

[4]Smith, T. F., Byun, K. H., and Chen, L. D., "Effects of Radiative and Conductive Transfer on Thermal Ignition," *Combustion and Flame*, Vol. 73, July 1988, pp. 67–74.

[5]Smith, T. F., and Chen, L.-D., "Effects of Radiative and Conductive Transfer on Thermal Ignition," *Handbook of Heat and Mass Transfer*, Vol. 4, Gulf Publishing Co., Houston, 1990, pp. 979–997.

[6]Field, M. A., Gill, D. W., Morgan, B. B., and Hawksley, P. G. W., *Combustion of Pulverized Coal*, BCURA, London, 1976, pp. 186–355.

[7]Baek, S. W., and Seung, S., "On the Postshock Flow Field of Carbon Particle Laden Gases," *Combustion and Flame*, Vol. 75, March 1989, pp. 255–263.

[8]Krazinski, J. L., Buckius, R. O., and Krier, H., "Coal Dust Flames: A Review and Development of a Model for Flame Propagation," *Progress in Energy Combustion Science*, Vol. 5, 1979, pp. 31–71.

[9]Baek, S. W., and Lee, C., "Heat Transfer in a Radiating Medium Between Flame and Fuel Surface," *Combustion and Flame*, Vol. 75, Feb. 1989, pp. 153–163.